20 and 30 m telescope designs with potential for subsequent incorporation into a track-mounted pair (20/20 or 30/30).

Roger Angel, Jim Burge, Johanan L. Codona, Warren Davison, and Buddy Martin
Steward Observatory, The University of Arizona

ABSTRACT

Any future giant ground-based telescope must, at a minimum, provide foci for seeing-limited imaging over a wide field and for diffraction-limited imaging over ~1 arcminute fields corrected by adaptive optics (AO). While this is possible with a number of design concepts, our choices are constrained if we anticipate wanting to later add a second telescope for imaging with still higher resolution, and very high contrast imaging for exoplanet studies. This paper explores designs that allow for such future development.

Higher resolution imaging by interferometric combination of the AO-corrected fields of two telescopes is possible without loss of point-source sensitivity or field of view, as long as the baseline can be held perpendicular to the source and varied in length. This requirement is made practical even for very large telescopes, provided both can move continuously on a circular track. The 20/20 telescope[1] illustrates this concept. Telescopes so mounted can additionally be operated as a Bracewell nulling interferometer with low thermal background, making possible the thermal detection of planets that would have been unresolvable by a single 20 m aperture.

In practice, limits set by funding and engineering experience will likely require a single 20 or 30 m telescope be built first. This would be on a conventional alt-az mount, but it should be at a site with enough room for later addition of a companion and track. In anticipation of future motion it should be compact and stiff, with a fast primary focal ratio. We envisage the use of large, highly aspheric, off-axis segments, manufactured using the figuring methods for strong asphercics already proven for 8 m class primaries. A compact giant telescope built under these guidelines should be able to perform well on its own for a broad range of astronomical observations, with good resistance to wind buffeting and simple alignment and control of its few, large segments. We compare here configurations with adjacent hexagonal segments and close-packed circular segments. For given segment parent size and number, the largest effective aperture is achieved if the segments are left as circles, when also the sensitivity and resolution for diffraction-limited operation with AO is higher. Large round segments can also be individually apodized for high-contrast imaging of exoplanets with the entire telescope–for example 8.4 m segments will yield 10^{-6} suppression 0.05 arcsec from a star at 1 μm wavelength, and 0.25 arcsec at 5 μm.

Keywords: giant telescopes, adaptive optics, apodization, high resolution imaging, extrasolar planets, Fizeau interferometer

1. INTRODUCTION

Current plans for future very large telescopes envisage apertures of 20 – 100 m diameter. Their gain over the present generation of 8 m telescopes will not be simply in proportion to their increased light gathering power. When corrected to the diffraction limit with adaptive optics, still higher sensitivity will be achieved because of the increased image sharpness.

Yet most plans fall short in one respect–they do not anticipate the coupling of additional telescopes to obtain still higher spatial resolution, by coherent beam combination as an interferometer. This is in contrast to the current generation of large telescopes, most of which were built in pairs (Keck, LBT, Magellan), or in the case of VLT as a group of four, with interferometric combination in mind.

It may seem unnecessary or even greedy to worry about multiple giant telescopes, when even one will be so much more powerful than what is now available. Surely, our efforts today must be focused on getting the first of these new giants funded and built. But if we envisage that at some later date an adjacent twin telescope might be built, then we need to allow for this now in the choice of site, and in the optical design and mounting. The accommodations needed in a single telescope to maximize scientific potential when used later in interferometric combination need not increase its cost or degrade performance, provided they are thought out ahead of time.

Future Giant Telescopes, J. Roger P. Angel, Roberto Gilmozzi, Editors,
Proceedings of SPIE Vol. 4840 (2003) © 2003 SPIE · 0277-786X/03/$15.00

We can be guided by the experience already developed with the VLT, Keck, and LBT interferometers, as well as smaller optical interferometers. Unfortunately, presently operating systems are small and limited to bright star observations. The enormous gain in sensitivity for interferometric imaging that will result when existing 8 m, AO-corrected elements are combined still lies in the future. We cannot yet point to major scientific results, but we do now understand the relative merits of the two fundamentally different approaches explored by these systems.

Most current interferometers including the VLT and Keck pair, fall into the first type, with separately mounted individual elements. Their beams are combined via a complex train of mirrors, with compensation for path length changes from Earth's rotation. This type has the advantage of long baseline, but is lossy, has high thermal background and a small field of view, often limited to the diffraction width of a single telescope. Imaging of complex objects suffers from incomplete u-v plane sampling. The second type, represented by the old MMT and the LBT, has elements on a single rigid mount with fixed, close spacing. These can take advantage of Fizeau beam combination geometry for interference over a large field of view, a fully sampled u-v plane, a high efficiency and low thermal background; but the rigid mounting results in no more than a factor of 3 improvement in resolution. Also co-mounted telescopes cannot be separately targeted, and instruments to work at the individual foci must be duplicated.

In a future interferometer with very large elements, we can combine the best features of both types by using just two large telescopes that are both mounted on a circular track allowing for continuous motion[1]. The idea of moving a thousand tons of telescope smoothly along a track may at first sight seem outlandish, until we remember that the whole telescope already has to move in rotation about a smaller horizontal azimuth track. Additional motion on hydrostatic bearings on the larger diameter track does not require any radical design change if the local azimuth rotation is already on such bearings. We envisage a pair of track-mounted 20 or 30 m telescopes as the end point of an evolution that would start with the construction of a single large telescope on a conventional alt-az mount. At a later date, a track with the second giant telescope mounted on it would be constructed and put into operation nearby. The first telescope would then be rebuilt on the track to form the second element. The telescopes would have separate alt-az mounts on the track, providing for continued independent operation when desired. An advantage of this scenario is that a smaller-scale test of the track-mounted concept can be made while the first telescope is built.

There are operational as well as scientific advantages in building large telescopes in pairs, even when they are operated quite independently, as is the case most of the time at the Keck, VLT, and Magellan Observatories. A full suite of individual instruments is not required for each telescope, and each instrument is used for a larger fraction of nights with fewer changes required.

This paper deals largely with the design of the first giant telescope that anticipates track motion later on. In the next section, we review the requirements for a pair of telescopes that are to be operated as a Fizeau interferometer. The remainder of the paper deals with design and performance of the single telescope element. To facilitate track motion this should be compact, i.e. have a short focal ratio primary. We explore optical designs with this constraint and consider how such primary mirrors might be synthesized from 8 m segments, and the effect of different geometries on diffraction and apodization for high-contrast imaging. Ways to manufacture, test, and control the alignment of such segments are then discussed in later papers in this session.[2,3] We also explore here how the reduction in diffracted halo needed for direct detection of exoplanets could be achieved by individual apodization of large, round segments.

2. COHERENT IMAGING WITH TRACK-MOUNTED TELESCOPES

Wide-field interferometric imaging with two telescopes on the same rigid mount was first demonstrated at the old MMT. The individual Cassegrain beams were combined as a Fizeau interferometer[4] with only two added reflections to create an exit pupil similar to the entrance pupil (figure 1a). The geometry is chosen so the rays forming the combined image satisfy the sine condition with respect to the entrance pupil. Then, if one star interferes coherently, so do nearby stars in the focal plane. All show the same high-resolution point spread function, the same as would be formed by a large aperture masked by a plate with openings corresponding to telescope elements. As an example, we show in figure 1b a K band image of the triple star γ And. During this long exposure, atmospherically induced fluctuations in path length and in wavefront slope (tip/tilt) were adaptively corrected from measurements of the primary star. The two images thus overlap, and the stabilized Young's fringes show clearly. The secondary and tertiary components lay 10 arcsec to the NE and are separated by 0.5 arcsec. Note that both components show the same PSF[5]. Similar images over AO corrected

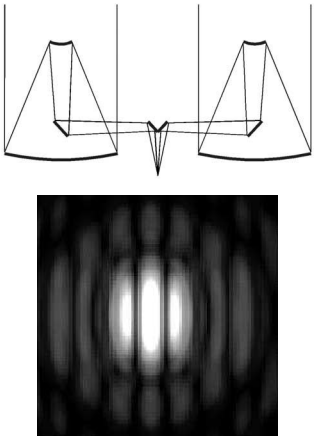

Figure1(a): Above: optical diagram for Fizeau beam combiner with co-mounted telescopes. Below: common achromatic PSF shown by all stars in the field

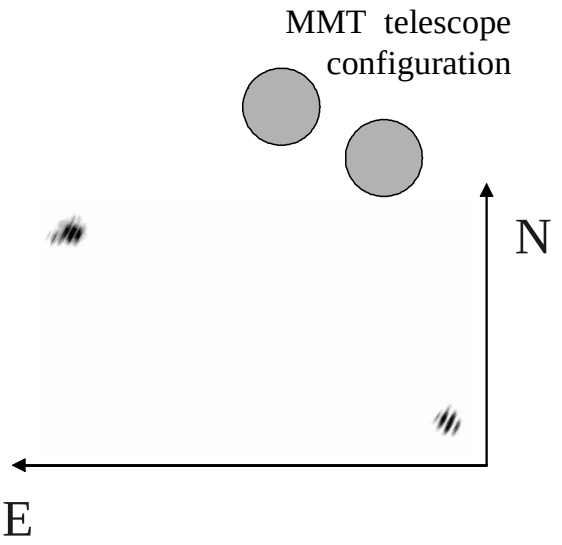

Figure 1(b): Single Fizeau exposure made with the old MMT, d=1.8 m, b=2.5 m. This K band image is of the triple star γ Andromeda. Young's fringes across the primary star are sensed and used to servo out atmospheric path errors. The secondary and tertiary stars, 10 arcsec to NE, separated by 0.5 arcsec, both show fringes in this long exposure.

fields up to 1 arcminute will be recorded with the Large Binocular Telescope (LBT), which has two 8.4 m telescopes rigidly co-mounted with 14.4 m between centers. Adaptive correction is made at the Gregorian secondary mirrors. Warm and cold beam combiner optics will form a coherent focus with an arcminute field of view, and the PSF shown in figure 3a.

High resolution images covering the full field of view corrected by single or multi-conjugate adaptive optics will be obtained by image reconstruction from a set of exposures obtained through the night at different baseline orientations. In general for a Fizeau interferometer, the resolution is the same as for as a filled-aperture telescope with a diameter equal to the longest baseline. This is shown in the simulation of imaging with the 20/20 concept by Hege and Close[1], reproduced in figure 2.

Two other points are important. First, when we compare the double to the single telescope, there is no loss of sensitivity to point sources or increased thermal background, in fact the limiting sensitivity is increased because of the increased aperture[6]. Second, the full fields that can be accessed for adaptive optics correction by the single telescope will also be accessible for higher resolution coherent imaging[1]. This is so because a field star is always required for AO: even when laser beacons are used a natural star is needed to sense wavefront tip/tilt. The same star will be bright enough to be used for phase reference, and the coherently phased field around it is as large as that corrected by the AO system. Since also very faint field stars in the infrared suffice to measure tip/tilt and phase at a diffraction-limited 20 m or larger telescope, most of the sky will be accessible, even at high galactic latitude.

A second type of coherent image combination will be valuable for direct detection of exoplanets. Here the greatest need for is not very high resolution, but very high contrast ratio. Because host stars are bright, accurate atmospheric wavefront correction and phase control should be possible with specially-optimized adaptive optics[7]. Thermal detection is then best accomplished by Bracewell nulling interferometry, in which the stellar wavefronts from two telescopes are overlapped with a 180-degree phase difference. They cancel out, while light from a nearby companion interferes constructively. This technique was also first demonstrated with two mirrors of the old MMT[8] and will be implemented on the adaptively corrected LBT with a cryogenic beam-combiner for very low thermal background[6]. For exoplanet imaging at thermal or optical wavelengths, it is crucial that the segmentation of the primary mirror is implemented in such a way that the diffracted halo caused by gaps or surface height steps can be minimized.

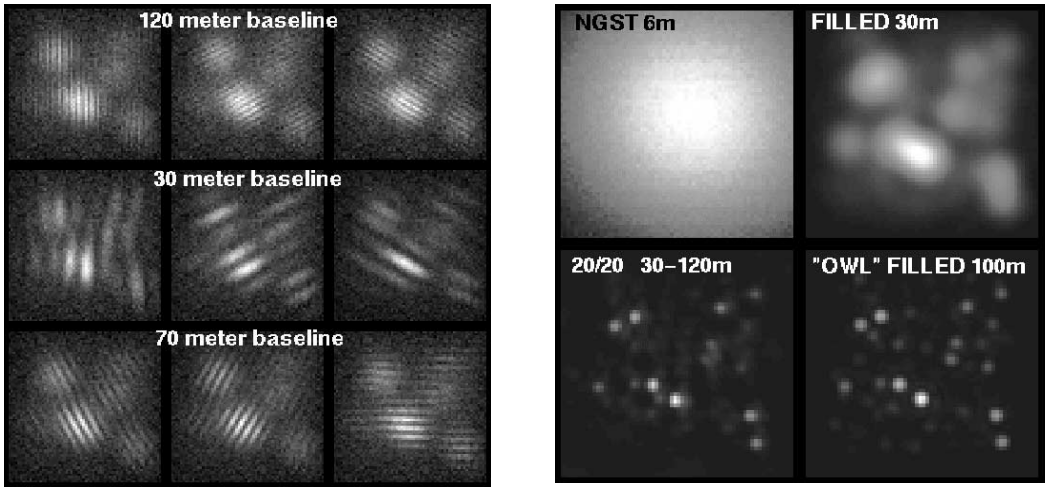

(a) **(b)**

Figure 2: (a) Detail of galactic bulge stars in simulated images of a cluster of galaxies at 100 Mpc. Each of the 9 exposures for this key project with the 20/20 telescope (3 orientations in each of three baselines) is 20 hours long. (b) Comparison of reconstructed image with those of 3 other telescopes (from ref 1). The full 20/20 image has 4 mas resolution over a 1 arcminute field, i.e. the richness of a Schmidt plate, and achieves 0.1 mag photometric accuracy at K'=29.

The 20/20 telescope concept[1] offers a way to configure a pair of large telescopes to fully realize the advantages of both independent and coherent operation. It consists of a pair of large telescopes with independent alt-az mounts, but with provision for continuous motion around a track when desired. In this way different baselines for interferometry can be chosen, while for any given baseline telescopes can be held perpendicular to the source while the baseline rotates during the night. This removes the need for lossy path length compensators, and satisfies the requirement for wide field Fizeau combination, which takes place at a station that tracks midway between. For much of the sky the u-v plane can be fully sampled for high resolution imaging of faint objects.

3. OPTICAL DESIGNS FOR COMPACT TELESCOPES

Any versatile large telescope must provide a variety of foci, for seeing and diffraction limited imaging over the wavelength range 0.3 – 30 μm. The seeing-limited focus should correct as wide a field as possible to the ¼ arcsec limit set by atmospheric seeing, and should be telecentric for convenience of operation with standardized integral field units. Single-conjugate AO correction will be valuable for small fields around natural guide stars, and for the thermal infrared where the smallest number of warm reflecting elements is needed. Multi-conjugate correction with laser guide stars is also needed, to correct fields of 1 arcminute when only faint field stars are available. In our case, looking ahead to operation as a Fizeau interferometer, we would like to incorporate as much of the single-telescope optical infrastructure into the optical train to the combined focus as possible.

Our base design is a compact Ritchey-Chretien or Gregorian system with adaptive secondary mirror. This yields highest throughput for both a substantial seeing-limited field and a single-conjugate AO corrected focus with low thermal background. MCAO correction, when needed, is made by the addition of a clamshell relay with adaptive elements. Alternative large telescope designs with built-in MCAO [9,10] use 4 – 6 mirrors, which in the case of OWL also provide correction for the primary spherical aberration. Our design, based on a two-mirror imaging system, has the advantage that for many applications no additional mirrors are required, and losses and thermal emission are minimized.

The adaptive secondary mirror is one-tenth the primary diameter and will form a focus at the direct Cassegrain or folded Nasmyth stations. It will use the technology developed for the MMT and LBT secondaries, in which the mirror surface can be used for complete AO correction, including tip/tilt, or set, if desired, to a predetermined static figure, by internal reference to a rigid ULE reference body, or used as an infrared chopping secondary[11]. Details of the design for MCAO for the individual 20 m telescopes of the 20/20 concept, and for optics to coherently combine the MCAO fields are given in ref 1. The design is based on a 22 m primary of 15 m focal length.

In recent work, Jim Burge has designed refractive correctors for seeing-limited, wide field foci for 20 and 30 m telescopes. He finds that for RC foci (as opposed to Gregorian) it is possible to design correctors whose glass elements are barely larger than the focal surface and are telecentric in the sense that the exit pupil is at the center of curvature of the curved focal plane[3]. Because the ray bundles are everywhere normal to the curved focal plane, multiple standard IFU/spectrograph units can be placed anywhere across the field. For a 30 m telescope with an f/0.5 primary and f/8 RC focus 15 m behind the primary vertex, the uncorrected field is 10 arc minutes wide with images ≤ 0.2 arcsec. The corrector with three 1.6 m fused silica elements yields a 20 arcminute, 1.5 m, telecentric focal surface with images ≤ 0.04 arcsec from 0.38 – 1.3 μm.

4. PRIMARY MIRRORS WITH 8.4 M SEGMENTS

We favor large segments for the primary mirror. These can be finished with the required highly aspheric, off-axis figure by methods already established for 8 m mirrors, which in today's large telescopes realize the best seeing-limited images and wavefront quality. We have explored several configurations with segments that are either 8.4 m diameter circles, or derived from them by cutting along chords. Figure 3b shows the initial segmentation concept for a 20/20 element[1] and 3d an extended concept for 30 m aperture with close fitting 8.4 m hexagonal segments, with the obscuration of the secondary and its supporting structure. (Details are given in table 1.) For a number of reasons we are also considering variants of these designs with full, round 8.4m segments, close-packed in rings of 6 or 18 with gaps of 0.25 or 0.4 m between segments, as shown in figures 3b and 3d. One reason is practical: hexagons are more time consuming to make than the circumscribing disc, and have smaller area. Another reason concerns the diffraction properties, as we discuss below. Concepts with a ring of 6 identical circular off-axis elements have also been explored by Kuhn et al[12]. Our designs are compared in table 2, which lists in column 1 the collecting area A and effective diameter, $2\sqrt{(A/\pi)}$.

Mechanical concepts for the 20 and 30 m telescopes with hexagonal segments have been worked out by Davison[13,14]. These designs are extremely stiff, with high resonant frequencies: the lowest, locked rotor frequency being 6.5 Hz for the 20 m version (fig. 3b) and 5.3 Hz for the 30 m (figs.3d & 4b). They could be readily adapted to the configurations with circular segments. For example, fig 4a is a concept for the ring of 6 circular segments of fig. 3c. It includes a secondary held by tension elements within a hexagonal cage that is hidden in the entrance pupil within the gaps around the central segment. The cage is supported by verticals that are hidden in the gaps between the 6 segments, and lies above the cone of rays converging from the primary to the 2 m adaptive secondary.

Each 8 m segment would be supported by a system similar to that used for current 8 m telescope mirrors. The six rigid-body degrees of freedom are set by a hexapod mount attached to "hard points" on the glass, while ~100 active flotation supports control large scale figure. These provide adjustments to compensate for gravitational flexure by maintaining

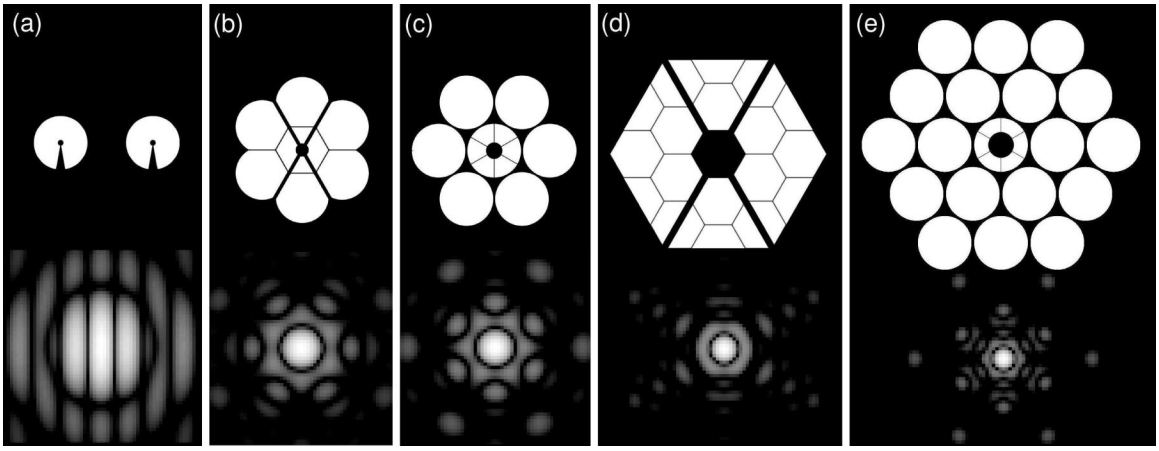

Figure 3: Pupil configurations for telescopes built up from 8.4 m segments. The corresponding point spread functions are shown below on a logarithmic gray scale covering 3 decades. Configuration (a) is the LBT, and the PSF is computed at its coherent, combined focus. Alternative seven-segment configurations are shown in (b) and (c), and 18 and 19 segment configurations in (d) and (e). At a reference wavelength of 1 μm, the FWHM of the LBT's central fringe is 7.2 mas (horizontal cut), while for the remaining radially averaged PSFs the FWHM are 11, 8.9, 7.2 and 5.3 mas respectively. More parameters are given in table 1.

Configuration *(label from figure 3)*	**Segment center-center spacing**	**Secondary mirror obstruction**	**Spider vane width**	**Crack width**
a	14.4 m	0.89 m	20° wedge	
b	7.28 m	2.0 m	0.25 m	0.05 m
c	8.65 m	2.5 m	0.012 m*	
d	7.28 m	8.4 m hex	1.0 m	0.05 m
e	8.8 m	4.0 m	0.012 m*	

Table 1. Details of configurations derived from 8.4 m segments showing spacings, spider vane, and crack widths. *center segment only

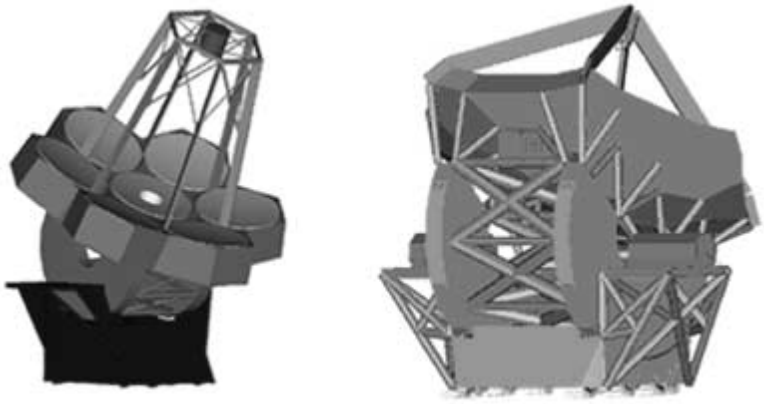

Figure 4: Mechanical designs for (a) 22-m f/0.8 (fig 3c); (b) 30-m f/0.5 (fig 3d).

the overall figure of the primary mirror and relative positions of the segments. The primary mirror displacements under gravity (with piston removed) amount to ~ 1 mm[13], well within the range of adjustment. To determine the adjustments, the segment positions and overall mirror figure would be monitored locally by mechanical or optical methods and globally via slope and phase measurements of field stars. In the case of the round segments, all six degrees of freedom that define the relative location of adjacent segments would be measured by mechanical or optical sensors bridging the segment gap.

Wind-driven tracking errors and disturbance of the primary mirror figure, though not major problems in current optical telescopes, becomes increasingly important with size. (The size limit to medieval cathedrals was set by wind, not gravity). For the modeled 20 and 30 m telescopes, wind causing a 100 Pa pressure load will cause ~ 10 μm displacement. This is small enough to lie within the dynamic range of the adaptive secondary mirror. The adaptive secondary will be segmented like the primary, so that any time-variable steps in the wavefront caused by differential motion of the primary segments will be corrected by equal and opposite steps at the boundaries of the secondary segments.

4.1 Seeing and diffraction-limited performance for the different configurations

For seeing-limited observations, the signal/noise ratio is proportional to the effective diameter. The relative performance of the four different pupil configurations is given in column 6 of table 2. For the same number of segments, the disc configurations are better because of their larger area. However, to realize this advantage for spectroscopy, the optics and gratings must be increased in size in proportion to the maximum pupil dimension (column 2).

When imaging at the diffraction limit with adaptive optics, the resolution increases in proportion to the pupil dimensions. Plots of the radially averaged PSFs and encircled energies for the different configurations for perfectly corrected wavefront are shown in figure 6a, b, e, and f, and the resolution given by the reciprocal of FWHM is given in column 4 of table 2. The fraction of total energy collected in the central peak (within the first dark ring) is reduced for the less-completely filled apertures, as shown in column 5. For detection of a faint point source against the photon noise from

the sky background in the diffraction limit, the S/N ratio varies as the source signal collected in the diffraction core, divided by the root of the sky signal in the same core, thus S/N $\propto f D_{eff}$ /FWHM. The S/N ratios, normalized to that of a single, unobscured 8.4 m disc, are listed in column 7. The configurations with full discs have better signal to noise ratio that those with fitted hexagons.

Configuration	Total area (m^2)	Effective diameter (m)	Circumscribing dimensions (m)	Resolution of diffraction core 1/FWHM (relative to 8.4m)	Energy fraction *f* encircled within diffraction core	S/N ratio improvement over 8.4 m disc	
						Seeing limited	Diffraction limited
8.4 m disc	55.4	8.4	8.4 x 8.4	1	0.84	1	1
b	340	20.8	21 x 22.95	2.61	0.74	2.4	5.6
c	379	22.0	23.6 x 26.0	2.90	0.68	2.6	6.2
d	615	28.0	33.6 x 29.1	3.78	0.66	3.3	9.9
e	1052	36.4	38.9 x 43.6	4.83	0.68	4.3	16.8

Table 2. Image characteristics and signal/noise ratio for various configurations.

5. MANUFACTURE OF LARGE, ASPHERIC SEGMENTS

The wide variety of different designs for very large telescopes now under consideration is largely due to different perceptions of the cost and difficulty of making primary mirror segments. In most concepts, optical losses, additional control complexity, and larger buildings are tolerated to avoid the highly aspheric segments needed for simple, compact, and efficient optics. But if such segments can be made at reasonable cost, then the total cost, reliability, and system performance could all be improved.

For our proposed telescopes, the large segments can be made using methods proven at the Mirror Lab in making the highest quality telescope mirrors. Since the aspheric departure over the 8.4 m segments only about an inch, the substrate discs can be cast while by spinning about their local axis, as for an axisymmetric 8.4 m mirror, but with a slightly thicker faceplate. Polishing can be by the stressed lap polishing technique developed at the Mirror Lab explicitly to handle highly aspheric surfaces–in particular the f/1.14 paraboloids of the LBT[2]. The polishing action is created by rotation of both the mirror and lap about their axes, while the lap is translated back and forth radially. As it moves, the lap is bent by computer-controlled actuators to conform to the local shape of the asphere, with updates made several hundred times/second. For off-axis segments, the same motions would be applied, with the segment rotated about its own local axis as usual, but the lap shape changes would be computed to fit the desired off-axis figure. The lap bending forces needed to figure 8 m segments of 20 and 30 m parents with 15 m focal length are similar to those already in use for the LBT[2], so the same lap can be used. Shop testing methods for the desired off-axis segments have been worked out[3].

5.1 Rate of production

More than a dozen glass substrates of 6.5 – 8.4 m diameter have been produced at the Mirror Lab and by Schott and Corning. The fourth and most recent 6.5 m honeycomb substrate cast at the Mirror Lab took 9 months. This period includes mold construction and the cycle of melting, annealing, and cooling–all in the same furnace. Optical finishing at 6.5 – 8.4 m diameter has evolved during the manufacture of 10 mirrors so far at the Mirror Lab and at REOSC in France. The 4 large mirrors figured to date at the Mirror Lab at f/1.25 and f/1.14 have been processed with a single 8 m vertical lathe, used for generation, loose abrasive grinding, and polishing. A second 8 m lathe has been purchased to double the production speed, so 8.4 m mirrors can be processed on a 9-month cycle to match the casting rate. This rate is consistent with REOSC's experience with two machines. Thus a set of 7 mirrors for a 20-22 m telescope would take ~6 years. For a set of 19 to be produced in less than 10 years, the Mirror Lab's entire current facility could be duplicated.

6. EXOPLANET DETECTION AND THE EFFECTS OF SEGMENTATION

Giant telescopes used both singly and in pairs will be capable of studying exoplanets by direct imaging and spectroscopy. Because planets are found very close to bright stars, accurate correction of atmospheric wavefront errors will be possible, for high-Strehl, diffraction-limited imaging.

The giant exoplanets we know are those with shorter periods and larger Doppler shifts. Given adequate resolution, they are also good candidates for direct detection, because they are illuminated and warmed by the star. In the current list of ~ 100 known exoplanets, about 25 have orbits > 1 AU, and will have maximum angular separations of typically ~0.05 arcsec. These are of especial interest because they lie in or near the habitable zone, and may show very strong water bands at $\lambda \sim 1$ μm. For example, υ And at 14 pc distance has giant planets in orbit at 0.83 and 2.5 AU (0.06 and 0.19 arcsec maximum extension). A recent detailed calculation of their expected spectra is shown in figure 5[15]. The predicted fluxes in the J band (1.25 μm) are about 3×10^{-8} of the F8V star. Detection and spectroscopy at this level will require extreme care to suppress the diffracted stellar halo, but should be possible.

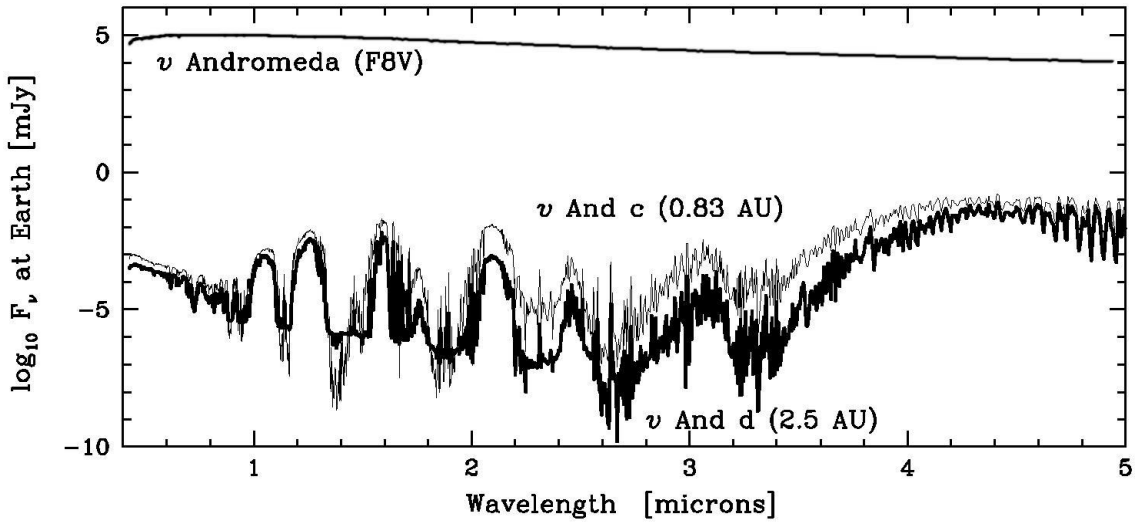

Figure 5: Theoretical visible and near-infrared spectra of υ And, and modeled spectra for the known c and d companions with Msini = 2.1 and 4.6 M_J. Courtesy D. Sudarsky, A. Burrows, and I. Hubeny.[15]

The fundamental limit to sensitivity to faint planets is set by photon noise in the halo underlying the planet. One contribution to this halo comes from residual wavefront errors after AO correction. For the bright stars in which we are interested, the limit set by photon noise in the wavefront sensor will result in a halo level ~ 10^{-6} of the central stellar peak[7]. Here we are concerned with the diffracted light halo component (in the absence of wavefront errors), which we would like to also hold at this level. Detection of a planet 100 times fainter than the instantaneous background level is still possible, provided the halo averages out to a smooth background during long exposures.

Thermal searches can be expected to yield discovery and spectroscopy of young giant planets at radii ~5 AU. This would open new discovery space for giant planets, those in large orbits where Doppler detection methods lose sensitivity because motions are of small amplitude and orbital periods > 5 years. The most favorable band is around 5 μm, where giant planets are expected to show a bright peak. Predicted 5 μm fluxes for isolated planets at 20 pc a billion years after formation vary from ~ 1 μJy for mass 1 M_J to ~100 μJy for mass 15 M_J [16]. The specific prediction for υ And at 14 pc from figure 6 is 10 μJy at 5 μm and ~3 μJy at 3.8 μm.

For the cleanest diffraction pattern and lowest thermal background, the ideal single telescope would have the entire primary mirror made as a continuous, off-axis surface, like the Greenbank radio telescope. This could be very efficiently apodized by tapering off the intensity of the last few meters at the edge, for high transmission and strong energy concentration in the central diffraction core. However, the technology for casting and polishing a monolith of 20-30 m size is not proven. The best alternative from the point of view of controlling the diffracted halo would have the same off-axis geometry, but with the entire surface synthesized from a completely regular pattern of small, close-fitting segments (10-20 cm). Stellar diffraction effects from the segment boundaries would then be largely restricted to a region beyond a radius of ~1 arcsec, leaving inside a search region which, when apodized in the same way as the continuous aperture, would be as clean. Apodization with high throughput can produce a very low diffracted halo at radii $\theta > 5\lambda/D$, i.e. for D=25 m and λ=1 μm, θ=40 mas, and at 5 μm θ=200 mas.

In practice, the technology for making and controlling and servicing so many very small segments is also not at an adequate level of maturity. The practical forms of segments and secondary support in an axisymmetric system discussed above will result in additional diffraction close to the star, but also some potential for correction. We report here some preliminary work looking at options for suppression by apodization at the segment level. Pupil masks would be applied at a reduced scale image of the entrance pupil, with different alternatives selected to provide reduction over specific survey regions. In practice, coronagraphs with field and Lyot stops will be used, allowing some improvement on the results given here for apodization alone.

The details of the faint outer parts of the diffraction patterns produced without apodization by the different configurations under consideration are shown in figure 6. The upper curve under each PSF shows in a log-log plot the radial average PSF extending from 1 mas to 1 arcsec with intensity down to 10^{-10}. The lower curve is the encircled energy plotted on a linear scale, again over the same range of 1 mas to 1 arcsec. We find that the diffracted halo strength at 1 μm without apodization is ~10^{-3} at 0.05 arcsec for both 7 segment configurations (figures 5a and b), ~5.10^{-4} for the 18 and 19 segments (figures 5e and f). Clearly some form of apodization is required to meet the 10^{-6} goal.

As is well known, the PSF for a telescope with repeated segments of the same shape is the convolution of the individual segment PSF with the "grating" pattern of points at the segment centers. This suggests a strategy for the round segment configurations in which we apply circularly symmetric apodization individually to the unobscured circular segments, and completely block the partially obscured central mirror. In this way, a circularly symmetric halo reduction can be realized, optimized for detection of a planet at known radius but unknown position angle.

Examples of PSFs for two different apodizations are shown in figure 6. Figures 6c and 6g show smooth shading chosen for high average throughput (50%), with transmission that tapers smoothly to the edges, but leaves the inner 4.4 m diameter unobscured. The intensity transmission is $\cos^4[(r-2.2)\pi/8]$ for $r>2.2$. In this case the radially-averaged PSF at 1 μm falls below 10^{-6} for radii > 200 mas (5c) and > 160 mas (5g).

To reach the known exoplanets we need strong reduction still closer to the star. This can be obtained over restricted zones with annular blocking masks that modify the individual segments' Airy patterns to produce a deep and broad dark ring[17]. For example, by blocking 40% of the aperture, in the annulus from radius 0.663 to 0.9, the halo level at 1 μm is brought $\leq 10^{-6}$ near 0.05 arcsec radius, as shown in figures 6d and 6h. Details are listed in table 3. The dark ring location can be increased with different mask geometries, chosen to search for a planet at known radius. (From the Doppler data, we can deduce the times and the angular radius of maximum extension, but not the position angle). Once a planet is detected, spectroscopic observations over many hours require suppression in a circle at the specific planet radius. For the 6 segment telescope with 65 m^2 effective collecting area in the image core, and 50% effective quantum efficiency, the sensitivity limit set by photon noise for J band detection of a planet at 10^{-8} of a 7.5 mag star would be 10σ for a 10,000 sec.

For infrared searches for self-luminous, young, or massive giant planets with a single giant telescope, the annular mask could be implemented at a pupil image in a cryogenic camera. The radius of the dark ring will scale with wavelength, and would thus be 0.19 arcsec at 3.8 μm and 0.25 arcsec at 5 microns at 20 pc. The S/N ratio relative to a single 8.4 m disc is given in the last column of table 2, figured from D_{eff}, *f*, and FWHM as given above. Scaling by these factors from the estimates of Gillett and Mountain[18] for the sky-noise limited sensitivity for a 10,000 sec integration with an 8 m telescope (10 σ), the limits for the 6 and 18 segment apodized telescopes in the same time would be 10 μJy and 2 μJy respectively at 5 μm and 1 and 0.2 μJy at 3.6 μm. They would thus be able to reach υ Andromeda c and d and to detect wide-orbit, giant planets in many young systems out to 20 pc. A telescope pair, operated as a Bracewell nulling interferometer, gains much more than a doubling in thermal sensitivity, as well as access to much closer orbits. Nulling is implemented so as to preserve true imaging, without relative field rotation[6]. Because the interference is at a semi-transparent beamsplitter that brings the two pupils into coincidence, it results in modulation according to source position on the sky, not in the focal plane fringes of Fizeau combination. The modulation is as $\sin^2(\pi\theta s/\lambda)$ where θ is the sourceangle on the sky from the central null fringe. It is not necessary to apodize the individual apertures, because entire diffraction patterns are suppressed. The residual transmission of the centered star depends on the angular size of its disc. Take, for example, observations of a solar twin at 20 pc made at 5 μm with the 32 m shortest baseline of a 20/20 configuration. The star will be suppressed by a factor 10^4. Constructive interference peaks showing as Airy patterns with all the energy from both telescopes will occur for sources located on the bright Young's fringes at ±16 mas, ±48 mas, ±80 mas etc. A strongly warmed giant planet at the first bright fringe (0.32 AU) would easily be detected against, and

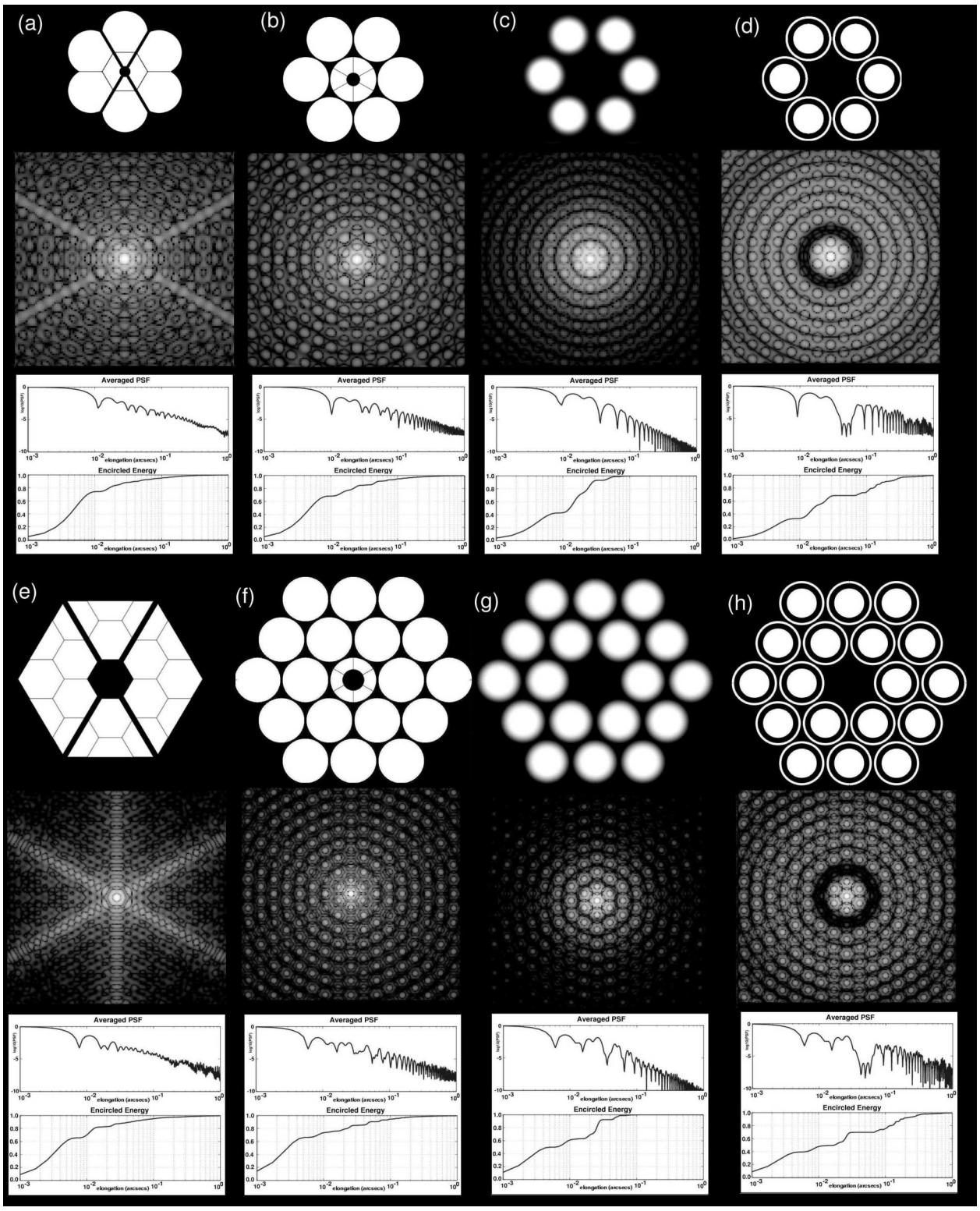

Figure 6: PSFs at 1 μm wavelength and covering a field of 0.4 arcsec on a side are shown for various pupils formed from 8.4m segments and with apodizing geometries as described in the text. The gray scale is logarithmic covering 7 decades. The dark rings in (d) and (h) at 10^{-6} of the stellar peak are at radius 0.05 arscsec. Shown below each psf are the average radial profiles to 10^{-10} of the stellar peak and the encircled energy, plotted against log angle from the central star. The horizontal scale runs from 10^{-3} to 1 arcsecs.

slightly displaced from, the central stellar diffraction peak reduced by 10^{-4}. One on the third peak, 1.6 AU from the star, would be seen against the first Airy ring of the star at a level ~10^{-6} of the full stellar peak. Because of the increased aperture and absence of apodization losses, the gain in sensitivity will approach an order of magnitude compared to the single telescope. This will allow detection and spectroscopy of many giant exoplanets.

ACKNOWLEDGEMENTS

This work has been supported by the NSF under grant AST-0138347 and AFOSR #F49620-01-1-0383.

REFERENCES

1. J.R.P. Angel, M. Lloyd-Hart, K. Hege, R. Sarlot, & C. Peng, "The 20/20 telescope: MCAO imaging at the individual and combined foci," *Beyond Conventional Adaptive Optics*, eds. R. Ragazzoni and S. Esposito, ESO, Venice, in press 2002.
2. H. M. Martin, J. R. P. Angel, J. H. Burge, S. M. Miller, J. M., Sasian, & P. A. Strittmatter, "Optics for the 20/20 telescope," *Future Giant Telescopes*, **4840**, SPIE, Kona, to be published 2002.
3. J. H. Burge and H. M. Martin, "Optical Issues for giant telescopes with extremely fast primary mirrors," *Future Giant Telescopes*, **4840**, SPIE, Kona, to be published 2002.
4. J. M. Beckers, E. K. Hege, & P. A. Strittmatter, "Optical interferometry with the MMT," *Advanced Technology Optical Telescopes II* , eds. L. D. Barr & B. Mack, **444**, pp. 85-92, SPIE, London, 1984.
5. M. Lloyd Hart & R Angel "Fizeau Interferometry of Gamma Andromeda" in preparation 2002.
6. P. M. Hinz, J. R. P. Angel, N. J. Woolf, W. F. Hoffmann & D. W McCarthy, Jr., "Imaging Extra-solar Systems from the Ground: The MMT and LBT Nulling Interferometers," *ASP Conference Series*, eds. S. Unwin & R. Stachnik **194**. pp.401, 1999.
7. J.R.P. Angel, "Imaging terrestrial exoplanets from the ground," *Scientific Frontiers in Research on Extrasolar Planets*, ed. D. Deming, *ASP*, Washington D.C., in press, 2002 and "Ground-Based Imaging of Extrasolar Planets Using Adaptive Optics," *Nature*, **368**, pp. 203-207, 1994.
8. P. M. Hinz, J. R. P. Angel, W. F. Hoffmann, D. W. McCarthy Jr., P. C. McGuire, M. Cheselka, J. L. Hora, & N. J. Woolf, "Imaging Circumstellar Environments with a Nulling Interferometer," *Nature*, **395**, pp. 251-253, 1998.
9. G. Brusa, A. Riccardi, M. Accardo, V. Biliotti, M. Carbillet, C. del Vecchio, S. Esposito, B. Femenía, O. Feeney, L. Fini, S. Gennari, L. Miglietta, P. Salinari, & P. Stefanini, "From adaptive secondary mirrors to extra-thin extra-large adaptive primary mirrors," in *Backaskog Workshop on Extremely Large Telescopes*, eds. T. Andersen, A. Ardeberg, & R. Gilmozzi, 57, p. 181, 2000.
10. R. Gilmozzi, P. Dierickx, & G. Monnet, "Science and Technology of a 100-m Telescope: The OWL Concept," in *Quasars, AGNs and Related Research Across 2000*, eds. G. Setti, & J. P. Swings, p. 184, Springer, 2001.
11. G. Brusa, A. Riccardi, P. Salinari, F. Wildi, M. Lloyd-Hart, H. Martin, R. Allen, D. Fisher, D. Miller, R. Biasi, D. Gallieni, and F. Zocchi, "MMT adaptive secondary: performance evaluation and field testing," *SPIE* **4839**, 2002.
12. J. R. Kuhn, G. Moretto, R. Racine, F. Roddier, and R. Coulter, "Concepts for a Large-Aperture, High Dynamic Range Telescope," *PASP*, **113**, pp. 1486-1510, 2001.
13. W. Davison & R. Angel, "Practical design of 20/20 and another 30 meter telescope," *Future Giant Telescopes*, **4840**, SPIE, Kona, to be published 2002.
14. W. Davison, N. Woolf, & R. Angel, "Design of track-mounted telescopes 20 and 30 m in diameter," *Future Giant Telescopes*, **4840**, SPIE, Kona, to be published 2002.
15. D. Sudarsky, A. Burrows, and I. Hubeny, "Theoretical Spectra and Atmospheres of Extrasolar Planets", submitted to *Ap.J.*, 2002.
16. A. Burrows, W. B. Hubbard, J. I. Lunine, and J. Liebert, "The theory of brown dwarfs and extrasolar giant planets," *Rev. Mod. Phys.* **73**, p. 719, 2001.
17. J. R. P. Angel, A. Y. S. Cheng and N. J. Woolf, "A Space Telescope for Infrared Spectroscopy of Earth-like Planets," *Nature* **322**, pp. 341-343, 1986.
18. F. Gillett & M. Mountain, "On the comparative performance of an 8 m NGST and a ground-based 8 m optical/IR telescope," *ASP conference series*, eds. E. Smith and A. Koratkar, **133**, pp. 42-52, 1997.